

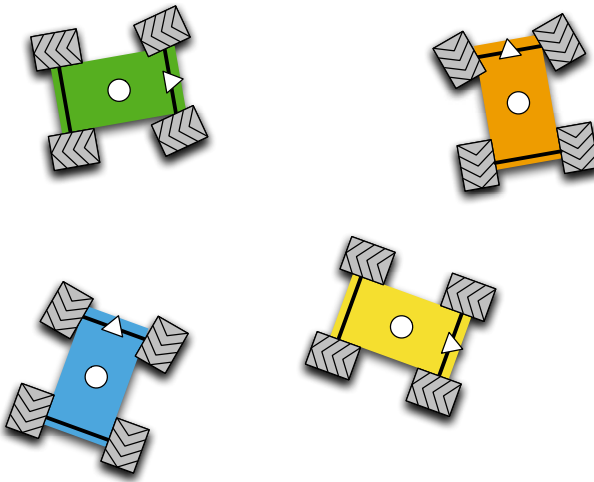
Distributed Control of Robotic Networks

A Mathematical Approach to Motion Coordination Algorithms

Chapter 5: Deployment

Francesco Bullo
Jorge Cortés
Sonia Martínez

May 20, 2009



PRINCETON UNIVERSITY PRESS
PRINCETON AND OXFORD

Copyright © 2006-2009 by F. Bullo, J. Cortés, and S. Martínez

This document is a complete free online version of the following book.

Distributed Control of Robotic Networks, by Francesco Bullo, Jorge Cortés and Sonia Martínez, Applied Mathematics Series, Princeton University Press, 2009, ISBN 978-0-691-14195-4.

The book is available online at

<http://coordinationbook.info>

- (i) You are allowed to freely download, share, print, or photocopy this document.
- (ii) You are not allowed to modify, sell, or claim authorship of any part of this document.
- (iii) We thank you for any feedback information, including suggestions, evaluations, error descriptions, or comments about teaching or research uses.

Contents

Chapter 5. Deployment	5
5.1 Problem statement	6
5.2 Deployment algorithms	8
5.3 Simulation results	19
5.4 Notes	23
5.5 Proofs	24
5.6 Exercises	31
Algorithm Index	39
Subject Index	41
Symbol Index	43

share May 20, 2009

Chapter Five

Deployment

The aim of this chapter is to present various solutions to the deployment problem. The *deployment objective* is to optimally place a group of robots in an environment of interest. The approach taken here consists of identifying aggregate functions that measure the quality of deployment of a given network configuration and designing control and communication laws that optimize these measures.

The variety of algorithms presented in the chapter stems from two causes. First, different solutions arise from the interplay between the spatially distributed character of the coordination algorithms and the limited sensing and communication capabilities of the robotic network. As an example, different solutions are feasible when agents have range-limited communication capabilities or when agents have omnidirectional line-of-sight visibility sensors. Second, there is no universal notion of deployment. Different scenarios give rise to different ways of measuring what constitutes a good deployment. As an example, a robotic network might follow a different strategy depending on whether or not it has information about areas of importance in the environment: in the first case, by incorporating the knowledge on the environment; or in the second, by assuming a worst-case scenario, where important things can be happening precisely at the furthest-away location from the network configuration.

Our exposition here follows [Cortés et al. \(2004, 2005\)](#), and [Cortés and Bullo \(2005\)](#). Our approach makes extensive use of the multicenter functions from geometric optimization introduced in Chapter 2. It is not difficult to synthesize continuous-time gradient ascent algorithms using the smoothness results presented in Section 2.3, and characterize their asymptotic convergence properties (as we ask the reader to do in Exercises E2.14 and E2.15). However, following the robotic network model of Chapter 3, we are interested in discrete-time algorithms. In general, gradient ascent algorithms implemented in discrete time require the selection of appropriate step sizes that guarantee the monotonic evolution of the objective function. This is usually accomplished via line search procedures, (see e.g., [Bertsekas and Tsitsiklis](#),

1997). In this chapter, we show that the special geometric properties of the multicenter functions and their gradients allow us to identify natural target locations for the robotic agents without the need to perform any line search.

The chapter is organized as follows. In the first section, we formally define the notions of deployment via task maps and multicenter functions. In the next section, we present motion coordination algorithms to achieve each deployment task. Specifically, we introduce control and communication laws based on various notions of geometric centers. We present convergence and complexity results for the proposed algorithms, along with simulations illustrating our analysis. The third section presents various simulations of the proposed motion coordination algorithms. We end the chapter with three sections on, respectively, bibliographic notes, proofs of the results presented in the chapter, and exercises. Throughout the exposition, we make extensive use of proximity graphs, multicenter functions, and geometric optimization. The convergence and complexity analyses are based on the LaSalle Invariance Principle and on linear dynamical systems defined by Toeplitz matrices.

5.1 PROBLEM STATEMENT

Here, we introduce various notions of deployment. We assume that $\mathcal{S} = (\{1, \dots, n\}, \mathcal{R}, E_{\text{cmm}})$ is a uniform robotic network, where the robots' physical state space is a (simple convex) polytope $Q \subset \mathbb{R}^d$ that describes an environment of interest. We define our notions of deployment relying upon the geometric optimization problems discussed in Section 2.3. Loosely speaking, we aim to deploy the robots in such a way as to optimize one of the multicenter functions, such as the expected-value multicenter function \mathcal{H}_{exp} , the disk-covering multicenter function \mathcal{H}_{dc} , or the sphere-packing multicenter function \mathcal{H}_{sp} . Indeed, these functions can be interpreted as quality-of-service measures for different scenarios. In order to formally define the task maps encoding the deployment objective, we take the following approach: since the optimizers of these measures are critical points, and these critical points are network configurations that make the gradients vanish, we define the task map to take the `true` value at these configurations.

5.1.1 The distortion, area, and mixed distortion-area deployment tasks

In this section, we define various notions of deployment originating from the expected-value multicenter function \mathcal{H}_{exp} . Recall the concepts of density and performance introduced in Section 2.3. Let $\phi : \mathbb{R}^d \rightarrow \mathbb{R}_{>0}$ be a density function on \mathbb{R}^d with support Q . One can interpret ϕ as a function measuring the probability that some event takes place over the environment. Let

$f : \mathbb{R}_{\geq 0} \rightarrow \mathbb{R}$ be a performance, that is, a non-increasing and piecewise differentiable function possibly with finite jump discontinuities. Performance functions describe the utility of placing a robot at a certain distance from a location in the environment. Here, we will restrict our attention to the cases $f(x) = -x^2$ (distortion problem), $f(x) = 1_{[0,a]}(x)$, $a \in \mathbb{R}_{>0}$ (area problem), and $f(x) = -x^2 1_{[0,a]}(x) - a^2 \cdot 1_{]a,+\infty[}(x)$, with $a \in \mathbb{R}_{>0}$ (mixed distortion-area problem).

For $\varepsilon \in \mathbb{R}_{>0}$, we define the ε -distortion deployment task $\mathcal{T}_{\varepsilon\text{-distor-dply}} : Q^n \rightarrow \{\text{true}, \text{false}\}$ by

$$\mathcal{T}_{\varepsilon\text{-distor-dply}}(P) = \begin{cases} \text{true}, & \text{if } \|p^{[i]} - \text{CM}_\phi(V^{[i]}(P))\|_2 \leq \varepsilon, i \in \{1, \dots, n\}, \\ \text{false}, & \text{otherwise,} \end{cases}$$

where $V^{[i]}(P)$ denotes the Voronoi cell of robot i , and $\text{CM}_\phi(V^{[i]}(P))$ denotes its centroid computed according to ϕ (see Section 2.1). In other words, $\mathcal{T}_{\varepsilon\text{-distor-dply}}$ is **true** for those network configurations where each robot is sufficiently close to the centroid of its Voronoi cell. According to Theorem 2.16, centroidal Voronoi configurations correspond to the critical points of the multicenter function $\mathcal{H}_{\text{dist}}$.

For $r, \varepsilon \in \mathbb{R}_{>0}$, we define the ε -r-area deployment task $\mathcal{T}_{\varepsilon\text{-r-area-dply}} : Q^n \rightarrow \{\text{true}, \text{false}\}$ as follows: we define $\mathcal{T}_{\varepsilon\text{-r-area-dply}}(P) = \text{true}$ whenever

$$\left\| \int_{V^{[i]}(P) \cap \partial \overline{B}(p^{[i]}, \frac{r}{2})} \mathbf{n}_{\text{out}}(q) \phi(q) dq \right\|_2 \leq \varepsilon, \quad i \in \{1, \dots, n\},$$

and we define $\mathcal{T}_{\varepsilon\text{-r-area-dply}}(P) = \text{true}$ otherwise. Here, the symbol \mathbf{n}_{out} denotes the outward normal vector to $\overline{B}(p^{[i]}, \frac{r}{2})$. In other words, $\mathcal{T}_{\varepsilon\text{-r-area-dply}}$ is **true** for those network configurations where each agent is sufficiently close to a local maximum for the area of its $\frac{r}{2}$ -limited Voronoi cell $V_{\frac{r}{2}}^{[i]}(P) = V^{[i]}(P) \cap \overline{B}(p^{[i]}, \frac{r}{2})$ at fixed $V^{[i]}(P)$. According to Theorem 2.16, the $\frac{r}{2}$ -limited area-centered Voronoi configurations correspond to the critical points of the multicenter function $\mathcal{H}_{\text{area}, \frac{r}{2}}$.

Finally, for $r, \varepsilon \in \mathbb{R}_{>0}$, we define the ε -r-distortion-area deployment task $\mathcal{T}_{\varepsilon\text{-r-distor-area-dply}} : Q^n \rightarrow \{\text{true}, \text{false}\}$ by

$$\begin{aligned} \mathcal{T}_{\varepsilon\text{-r-distor-area-dply}}(P) \\ = \begin{cases} \text{true}, & \text{if } \|p^{[i]} - \text{CM}_\phi(V_{\frac{r}{2}}^{[i]}(P))\|_2 \leq \varepsilon, i \in \{1, \dots, n\}, \\ \text{false}, & \text{otherwise.} \end{cases} \end{aligned}$$

In other words, $\mathcal{T}_{\varepsilon\text{-r-distor-area-dply}}$ is **true** for those network configurations where each robot is sufficiently close to the centroid of its $\frac{r}{2}$ -limited Voronoi cell. According to Theorem 2.16, $\frac{r}{2}$ -limited centroidal Voronoi configurations

are the critical points of the multicenter function $\mathcal{H}_{\text{dist-area}, \frac{r}{2}}$.

5.1.2 The disk-covering and sphere-packing deployment tasks

Here, we provide two additional notions of deployment based on the multicenter functions \mathcal{H}_{dc} and \mathcal{H}_{sp} , respectively.

For $\varepsilon \in \mathbb{R}_{>0}$, the ε -disk-covering deployment task $\mathcal{T}_{\varepsilon\text{-dc-dply}} : Q^n \rightarrow \{\text{true}, \text{false}\}$ is defined as

$$\mathcal{T}_{\varepsilon\text{-dc-dply}}(P) = \begin{cases} \text{true}, & \text{if } \|p^{[i]} - \text{CC}(V^{[i]}(P))\|_2 \leq \varepsilon, i \in \{1, \dots, n\}, \\ \text{false}, & \text{otherwise,} \end{cases}$$

where $\text{CC}(V^{[i]}(P))$ denotes the circumcenter of the Voronoi cell of robot i . In other words, $\mathcal{T}_{\varepsilon\text{-dc-dply}}$ is **true** for those network configurations where each robot is sufficiently close to the circumcenter of its Voronoi cell. According to Section 2.3.2, circumcenter Voronoi configurations are, under certain technical conditions, critical points of the multicenter function \mathcal{H}_{dc} .

For $\varepsilon \in \mathbb{R}_{>0}$, the ε -sphere-packing deployment task $\mathcal{T}_{\varepsilon\text{-sp-dply}} : Q^n \rightarrow \{\text{true}, \text{false}\}$ is defined as

$$\mathcal{T}_{\varepsilon\text{-sp-dply}}(P) = \begin{cases} \text{true}, & \text{if } \text{dist}_2(p^{[i]}, \text{IC}(V^{[i]}(P))) \leq \varepsilon, i \in \{1, \dots, n\}, \\ \text{false}, & \text{otherwise,} \end{cases}$$

where $\text{IC}(V^{[i]}(P))$ denotes the incenter set of the Voronoi cell of robot i . In other words, $\mathcal{T}_{\varepsilon\text{-sp-dply}}$ is **true** for those network configurations where each robot is sufficiently close to the incenter set of its Voronoi cell. According to Section 2.3.3, incenter Voronoi configurations are, under certain technical conditions, critical points of the multicenter function \mathcal{H}_{sp} .

5.2 DEPLOYMENT ALGORITHMS

In this section, we present algorithms that can be used by a robotic network to achieve the various notions of deployment introduced in the previous section. Throughout the discussion, we use the uniform networks \mathcal{S}_D and \mathcal{S}_{LD} of locally connected first-order agents with the Delaunay and r -limited Delaunay communication, respectively, introduced in Example 3.4, and the uniform network $\mathcal{S}_{\text{vehicles}}$ of planar vehicle robots with Delaunay communication introduced in Example 3.5. The networks \mathcal{S}_D and \mathcal{S}_{LD} evolve in a polytope $Q \subset \mathbb{R}^d$, while the network $\mathcal{S}_{\text{vehicles}}$ evolves in a convex polygon $Q \subset \mathbb{R}^2$. For all the laws presented in this chapter, we assume that no two agents are initially at the same position, i.e., we assume that the initial

network configuration always belongs to $Q^n \setminus \mathcal{S}_{\text{coinc}}$, where n denotes the number of robots.

All the laws presented in this chapter share a similar structure, which we loosely describe as follows:

[Informal description] In each communication round, each agent performs the following tasks: (i) it transmits its position and receives its neighbors' positions; (ii) it computes a notion of the geometric center of its own cell, determined according to some notion of partition of the environment. Between communication rounds, each robot moves toward this center.

The notions of geometric center and of partition of the environment are different for each algorithm, and specifically tailored to the deployment task at hand. Let us examine them for each case.

5.2.1 Geometric-center laws

We present control and communication laws defined on the network \mathcal{S}_D . All the laws share in common the use of the notion of Voronoi partition of the environment Q . We first introduce the VRN-CNTRD law, which makes use of the notion of the centroid of a Voronoi cell. We then propose two sets of variations to this law. First, we present the VRN-CNTRD-DYNMCS law, which implements the same centroid strategy on a network of planar vehicles. Second, we introduce the VRN-CRCMCNTR and VRN-NCNTR laws, which instead make use of the notions of the circumcenter and incenter of a Voronoi cell, respectively.

5.2.1.1 Voronoi-centroid control and communication law

Here, we define the VRN-CNTRD control and communication law for the network \mathcal{S}_D , which we denote by $\mathcal{CC}_{\text{VRN-CNTRD}}$. This law was introduced by [Cortés et al. \(2004\)](#). We formulate the algorithm using the description model of Chapter 3. The law is uniform, static, and data-sampled, with standard message-generation function. (Recall from Definition 3.9 and Remark 3.11 that a control and coordination law (1) is uniform if processor state set, message-generation, state-transition and control functions are the same for each agent; (2) is static if the processor state set is a singleton, i.e., the law requires no memory; (3) is data-sampled if the control functions

are independent of the current position of the robot and depend only upon the robots position at the last sample time.)

Robotic Network: \mathcal{S}_D with discrete-time motion model (4.1.1)
in Q , with absolute sensing of own position

Distributed Algorithm: VRN-CNTRD

Alphabet: $\mathbb{A} = \mathbb{R}^d \cup \{\text{null}\}$

function $\text{msg}(p, i)$

1: **return** p

function $\text{ctl}(p, y)$

1: $V := Q \cap (\bigcap \{H_{p, p_{\text{rcvd}}} \mid \text{for all non-null } p_{\text{rcvd}} \in y\})$

2: **return** $\text{CM}_\phi(V) - p$

Recall that $H_{p,x}$ is the half-space of points q in \mathbb{R}^d with the property that $\|q-p\|_2 \leq \|q-x\|_2$. Since the centroid of a Voronoi cell belongs to the interior of the cell itself, if the robots are at distinct locations at any one time, then they are at distinct locations after one step. Therefore, the set $Q^n \setminus \mathcal{S}_{\text{coinc}}$ is positively invariant with respect to the control and communication law $\mathcal{CC}_{\text{VRN-CNTRD}}$. Moreover, note that the direction of motion specified by the control function ctl coincides with the gradient of the distortion multicenter function $\mathcal{H}_{\text{dist}}$. Hence, this law prescribes a gradient ascent strategy for each robot that, as we will show later, monotonically optimizes $\mathcal{H}_{\text{dist}}$.

5.2.1.2 Voronoi-centroid law on planar vehicles

Next, we provide an interesting variation of the VRN-CNTRD law defined on the network $\mathcal{S}_{\text{vehicles}}$. Accordingly, we adopt the continuous-time motion model for the unicycle vehicle:

$$\begin{aligned}\dot{p}^{[i]}(t) &= v^{[i]}(t) (\cos(\theta^{[i]}(t)), \sin(\theta^{[i]}(t))), \\ \dot{\theta}^{[i]}(t) &= \omega^{[i]}(t), \quad i \in \{1, \dots, n\},\end{aligned}\tag{5.2.1}$$

where we assume that forward and angular velocities are upper bounded. We refer to this control and communication law as the VRN-CNTRD-DYNMCS law, and we denote it by $\mathcal{CC}_{\text{VRN-CNTRD-DYNMCS}}$. The law was introduced by [Cortés et al. \(2004\)](#) and is uniform and static, but not data-sampled:

Robotic Network: $\mathcal{S}_{\text{vehicles}}$ with motion model (5.2.1) in Q ,
with absolute sensing of own position

Distributed Algorithm: VRN-CNTRD-DYNMCS

Alphabet: $\mathbb{A} = \mathbb{R}^2 \cup \{\text{null}\}$

function $\text{msg}((p, \theta), i)$

1: **return** p

function $\text{ctl}((p, \theta), (p_{\text{smpd}}, \theta_{\text{smpd}}), y)$

1: $V := Q \cap (\bigcap \{H_{p_{\text{smpd}}, p_{\text{rcvd}}} \mid \text{for all non-null } p_{\text{rcvd}} \in y\})$

2: $v := k_{\text{prop}} |(\cos \theta, \sin \theta) \cdot (p - \text{CM}_\phi(V))|$

3: $\omega := 2k_{\text{prop}} \arctan \frac{(-\sin \theta, \cos \theta) \cdot (p - \text{CM}_\phi(V))}{(\cos \theta, \sin \theta) \cdot (p - \text{CM}_\phi(V))}$

4: **return** (v, ω)

This algorithm is illustrated in Figure 5.1.

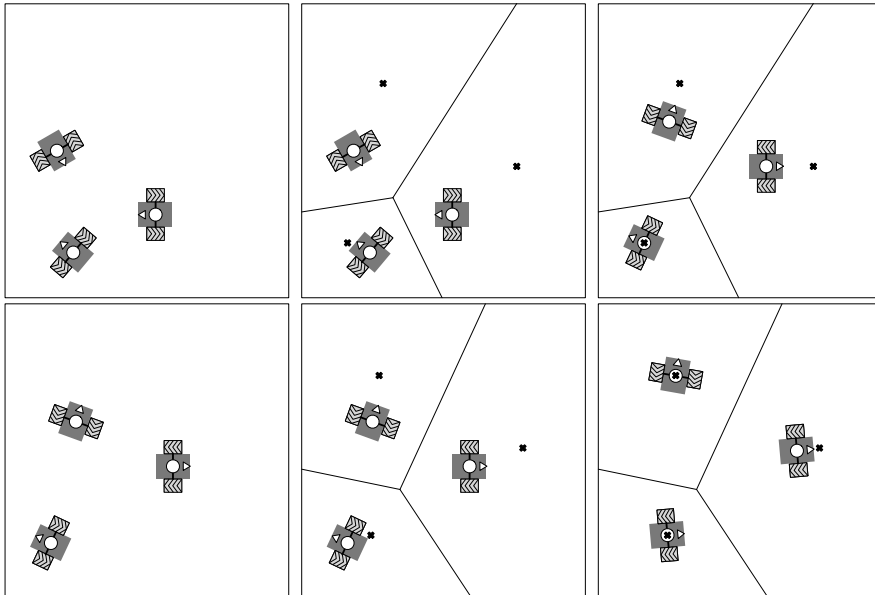


Figure 5.1 An illustration of the execution of VRN-CNTRD-DYNMCS. Each row of plots represents an iteration of the law. In each round, each agent first computes its Voronoi cell, then determines the centroid, and then moves towards it.

In the above description, we require the feedback gain k_{prop} to belong to the interval $]0, \frac{1}{\max\{\pi, \text{diam}(Q)\}}]$. This guarantees that the controls v, ω in the definition of ctl belong to the closed interval $[-1, 1]$, and are therefore, implementable in the unicycle and the differential drive robot models.

The definition of the control function ctl is based on the stabilizing feedback law of Astolfi (1999). When following this control law, the robot posi-

tion p is guaranteed to monotonically approach the target position $\text{CM}_\phi(V)$. Unfortunately, it is a only conjecture that this controller (or an appropriately modified controller) does not lead two agents to the same positions (indeed, it is possible that an agent move outside its Voronoi cell). Under this conjecture, the VRN-CNTRD-DYNMCS law enjoys the same convergence guarantees as the VRN-CNTRD law, that are described in Theorem 5.5.

Remark 5.1 (Vehicles with general dynamics). The general idea of moving towards the centroid of a robot's Voronoi region can be implemented over a network of vehicles with arbitrary dynamics, as long as these vehicles are capable of strictly decreasing the distance to any specified position in Q in the time intervals between communication rounds while remaining inside their Voronoi cells. •

5.2.1.3 Voronoi-circumcenter control and communication law

Here, we define the VRN-CRCMCNTR control and communication law for the network \mathcal{S}_D , which we denote by $\mathcal{CC}_{\text{VRN-CRCMCNTR}}$. This law was introduced by [Cortés and Bullo \(2005\)](#). The law is uniform, static, and data-sampled, with standard message-generation function:

Robotic Network: \mathcal{S}_D with discrete-time motion model (4.1.1)
in Q , with absolute sensing of own position

Distributed Algorithm: VRN-CRCMCNTR

Alphabet: $\mathbb{A} = \mathbb{R}^d \cup \{\text{null}\}$

```

function msg( $p, i$ )
  1: return  $p$ 

function ctl( $p, y$ )
  1:  $V := Q \cap (\bigcap \{H_{p, p_{\text{rcvd}}} \mid \text{for all non-null } p_{\text{rcvd}} \in y\})$ 
  2: return CC( $V$ ) -  $p$ 

```

Note that the circumcenter of a Voronoi cell belongs to the cell itself and therefore, robots evolving under the control and communication law $\mathcal{CC}_{\text{VRN-CRCMCNTR}}$ never leave the set Q . However, in general the set $Q^n \setminus \mathcal{S}_{\text{coinc}}$ is not positively invariant, see Exercise E5.1. From a geometric perspective, this law makes sense as a strategy to optimize the disk-covering multicenter function \mathcal{H}_{dc} . From Section 2.1.3, for fixed V , the circumcenter location minimizes the cost given by the maximum distance to all points in V . From Section 2.3.2, \mathcal{H}_{dc} can be expressed (2.3.12) as the maximum over the network of each robot's individual cost.

5.2.1.4 Voronoi-incenter control and communication law

Here, we define the VRN-NCNTR control and communication law for the network \mathcal{S}_D , which we denote by $\mathcal{CC}_{\text{VRN-NCNTR}}$. This law was introduced by [Cortés and Bullo \(2005\)](#). The law is uniform, static, and data-sampled, with standard message-generation function:

Robotic Network: \mathcal{S}_D with discrete-time motion model (4.1.1)
in Q , with absolute sensing of own position

Distributed Algorithm: VRN-NCNTR

Alphabet: $\mathbb{A} = \mathbb{R}^d \cup \{\text{null}\}$

```

function msg( $p, i$ )
  1: return  $p$ 

function ctl( $p, y$ )
  1:  $V := Q \cap (\bigcap \{H_{p, p_{\text{rcvd}}} \mid \text{for all non-null } p_{\text{rcvd}} \in y\})$ 
  2: return  $x \in \text{IC}(V) - p$ 

```

Since the incenter set of a Voronoi cell belongs to the interior of the cell itself, if the robots are at distinct locations at any one time, then they are at distinct locations after one step. That is, the set $Q^n \setminus \mathcal{S}_{\text{coinc}}$ is positively invariant with respect to the control and communication law $\mathcal{CC}_{\text{VRN-NCNTR}}$. From a geometric perspective, this law makes sense as a strategy for optimizing the sphere-packing multicenter function \mathcal{H}_{sp} . From Section 2.1.3, for fixed V , the incenter locations maximize the cost given by the minimum distance to the boundary of V . From Section 2.3.3, \mathcal{H}_{sp} can be expressed (2.3.15) as the minimum over the network of each robot's individual cost.

Remark 5.2 (“Move-toward-furthest-vertex” and “away-from-closest-neighbor” coordination algorithms). Consider the coordination algorithm where, at each time step, each robot moves towards the furthest-away vertex of its own Voronoi cell. Alternatively, consider the coordination algorithm where, at each time step, each robot moves away from its closest neighbor. Both coordination algorithms define maps which depend discontinuously on the robots' positions. [Cortés and Bullo \(2005\)](#) study the asymptotic behavior of these laws, and show that the “move-toward-furthest-vertex” algorithm monotonically optimizes the multicenter function \mathcal{H}_{dc} , while the “away-from-closest-neighbor” algorithm monotonically optimizes the multicenter function \mathcal{H}_{sp} . •

5.2.2 Geometric-center laws with range-limited interactions

In the following, we present two control and communication laws on the network \mathcal{S}_{LD} . Both laws prescribe a geometric centering strategy for each robot and accomplish specific forms of expected-value optimization. The LMTD-VRN-NRML law optimizes the area multicenter function $\mathcal{H}_{\text{area}, \frac{r}{2}}$, while the LMTD-VRN-CNTRD law optimizes the mixed distortion-area multicenter function $\mathcal{H}_{\text{dist-area}, \frac{r}{2}}$.

5.2.2.1 Limited-Voronoi-normal control and communication law

Here, we define the LMTD-VRN-NRML control and communication law for the network \mathcal{S}_{LD} . This law was introduced by [Cortés et al. \(2005\)](#). The LMTD-VRN-NRML law, which we denote by $\mathcal{CC}_{\text{LMTD-VRN-NRML}}$, uses the notion of $\frac{r}{2}$ -limited Voronoi partition inside Q . The law is uniform, static, and data-sampled, with standard message-generation function:

Robotic Network: \mathcal{S}_{LD} with discrete-time motion model (4.1.1)
with absolute sensing of own position, and
with communication range r , in Q

Distributed Algorithm: LMTD-VRN-NRML

Alphabet: $\mathbb{A} = \mathbb{R}^d \cup \{\text{null}\}$

function $\text{msg}(p, i)$

1: **return** p

function $\text{ctl}(p, y)$

1: $V := Q \cap (\bigcap \{H_{p, p_{\text{recv}}} \mid \text{for all non-null } p_{\text{recv}} \in y\})$

2: $v := \int_{V \cap \partial \overline{B}(p, \frac{r}{2})} n_{\text{out}}(q) \phi(q) dq$

3: $\lambda_* := \max \left\{ \lambda \mid \delta \mapsto \int_{V \cap \overline{B}(p + \delta v, \frac{r}{2})} \phi(q) dq \text{ is strictly increasing on } [0, \lambda] \right\}$

4: **return** $\lambda_* v$

In the above algorithm, n_{out} denotes the outward normal vector to $\overline{B}(p, \frac{r}{2})$. Note that the direction of motion v specified by the control function ctl coincides with the gradient of the multicenter function $\mathcal{H}_{\text{area}, \frac{r}{2}}$. The parameter λ_* corresponds to performing a line search procedure along the direction of the vector v .

The control function has the property that the point $p + \text{ctl}(p, y)$ is guaranteed to be in the interior of V . This can be justified by noting that for fixed V , the gradient of the function $p \rightarrow \int_{V \cap \overline{B}(p, \frac{r}{2})} \phi(q) dq$ at points in the boundary of V is non-vanishing and points toward the interior of V (cf. Exercise E2.5). As a consequence, the line search procedure terminates before reaching the boundary of V . This discussion guarantees that the set $Q^n \setminus \mathcal{S}_{\text{coinc}}$ is positively invariant with respect to the control and communication law $\mathcal{CC}_{\text{LMTD-VRN-NRML}}$.

5.2.2.2 Limited-Voronoi-centroid control and communication law

Here, we define the LMTD-VRN-CNTRD control and communication law for the network \mathcal{S}_{LD} . This law was introduced by Cortés et al. (2005). The LMTD-VRN-CNTRD law, which we denote by $\mathcal{CC}_{\text{LMTD-VRN-CNTRD}}$, uses the notion of $\frac{r}{2}$ -limited Voronoi partition inside Q and of centroid of the individual $\frac{r}{2}$ -limited Voronoi cells. The law is uniform, static, and data-sampled, with standard message-generation function:

Robotic Network: \mathcal{S}_{LD} with discrete-time motion model (4.1.1)
with absolute sensing of own position, and
with communication range r , in Q

Distributed Algorithm: LMTD-VRN-CNTRD

Alphabet: $\mathbb{A} = \mathbb{R}^d \cup \{\text{null}\}$

function $\text{msg}(p, i)$

1: **return** p

function $\text{ctl}(p, y)$

1: $V := Q \cap \overline{B}(p, \frac{r}{2}) \cap (\bigcap \{H_{p, p_{\text{recv}}} \mid \text{for all non-null } p_{\text{recv}} \in y\})$
2: **return** $\text{CM}_\phi(V) - p$

The centroid of a $\frac{r}{2}$ -limited Voronoi cell belongs to the interior of the cell itself, and this fact guarantees that the set $Q^n \setminus \mathcal{S}_{\text{coinc}}$ is positively invariant with respect to the control and communication law $\mathcal{CC}_{\text{LMTD-VRN-CNTRD}}$. Moreover, note that the direction of motion specified by the control function ctl coincides with the gradient of the multicenter function $\mathcal{H}_{\text{dist-area}, \frac{r}{2}}$.

Remark 5.3 (Relative sensing version). It is possible to implement the limited-Voronoi-normal and limited-Voronoi-centroid laws as static relative-sensing control laws on the relative-sensing network $\mathcal{S}_{\text{disk}}^{\text{rs}}$. This is a consequence of the fact that the r -limited Delaunay graph is spatially distributed

over the r -disk graph (cf., Theorem 2.7(iii)). Let us present one of these examples for completeness:

Relative Sensing Network: $\mathcal{S}_{\text{disk}}^{\text{rs}}$ with motion model (4.1.2)
 in Q , no communication, relative sensing for robot i given by:
 robot measurements y contains $p_i^{[j]} \in \overline{B}(\mathbf{0}_2, r)$ for all $j \neq i$
 environment measurement is $y_{\text{env}} = (Q_\varepsilon)_i \cap \overline{B}(\mathbf{0}_d, r)$

Distributed Algorithm: RELATIVE-SENSING LMTD-VRN-CNTRD

```
function ctl( $y, y_{\text{env}}$ )
1:  $V := y_{\text{env}} \cap \overline{B}(\mathbf{0}_d, \frac{r}{2}) \cap (\bigcap \{H_{\mathbf{0}_d, p_{\text{snsd}}} \mid \text{for all non-null } p_{\text{snsd}} \in y\})$ 
2: return  $\text{CM}_\phi(V)$ 
```

Note that only the positions of neighboring robots in the r -limited Delaunay graph have an effect on the computation of the set V . •

Remark 5.4 (Range-limited version of Vrn-cntrd). The LMTD-VRN-NRML and LMTD-VRN-CNTRD laws can be combined into a single control and communication law to synthesize an algorithm that monotonically optimizes the function $\mathcal{H}_{\text{dist-area}, \frac{r}{2}, b}$, with $b = -\text{diam}(Q)^2$. This law, which we term RNG-VRN-CNTRD, is uniform, static, and data-sampled, with standard message-generation function:

Robotic Network: \mathcal{S}_{LD} with discrete-time motion model (4.1.1)
 in Q , with absolute sensing of own position, and
 with communication range r

Distributed Algorithm: RNG-VRN-CNTRD

Alphabet: $\mathbb{A} = \mathbb{R}^d \cup \{\text{null}\}$

```
function msg( $p, i$ )
1: return  $p$ 

function ctl( $p, y$ )
1:  $V := Q \cap (\bigcap \{H_{p, p_{\text{rcvd}}} \mid \text{for all non-null } p_{\text{rcvd}} \in y\})$ 
2:  $v_1 := 2 \text{A}_\phi(V \cap \overline{B}(p, \frac{r}{2}))(\text{CM}_\phi(V \cap \overline{B}(p, \frac{r}{2})) - p)$ 
3:  $v_2 := (\text{diam}(Q)^2 - \frac{r^2}{4}) \int_{V \cap \partial \overline{B}(p, \frac{r}{2})} n_{\text{out}}(q) \phi(q) dq$ 
4:  $\lambda_* := \max \left\{ \lambda \mid \delta \mapsto \mathcal{H}_V(p + \delta(v_1 + v_2), \overline{B}(p + \delta(v_1 + v_2), \frac{r}{2})) \right.$ 
      is strictly increasing on  $(0, \lambda)$ 
5: return  $\lambda_*(v_1 + v_2)$ 
```

In the above algorithm, \mathbf{n}_{out} denotes the outward normal vector to $\overline{B}(p, \frac{r}{2})$ and, for a point $p \in V$ and a closed ball \overline{B} centered at a point in V with radius $\frac{r}{2}$, \mathcal{H}_V is defined as

$$\mathcal{H}_V(p, \overline{B}) = - \int_{V \cap \overline{B}} \|q - p\|_2^2 \phi(q) dq - \text{diam}(Q)^2 \int_{V \cap (Q \setminus \overline{B})} \phi(q) dq.$$

The RNG-VRN-CNTRD law is relevant because of the following discussion. Recall from Proposition 2.17 that the general mixed distortion-area multicenter function can be used to provide constant-factor approximations of the distortion function $\mathcal{H}_{\text{dist}}$. As we discussed in Section 2.3.1, robots with range-limited interactions cannot implement VRN-CNTRD because, for a given $r \in \mathbb{R}_{>0}$, \mathcal{G}_D is not in general spatially distributed over $\mathcal{G}_{\text{disk}}(r)$ (cf., Remark 2.10). However, robotic agents with range-limited interactions can implement the computations involved in LMTD-VRN-NRML and LMTD-VRN-CNTRD, and hence can optimize $\mathcal{H}_{\text{dist-area}, \frac{r}{2}, b}$, with $b = -\text{diam } Q^2$. Assuming $r \leq 2 \text{diam}(Q)$, it is fair to say that the above algorithm can be understood as a range-limited version of the VRN-CNTRD law. •

5.2.3 Correctness and complexity of geometric-center laws

In this section, we characterize the convergence and complexity properties of the geometric-center laws. The asynchronous execution of the Voronoi-centroid control and communication law can be studied as an asynchronous gradient dynamical system (see Cortés et al., 2004).

The following theorem summarizes the results known in the literature about the asymptotic properties of these laws.

Theorem 5.5 (Correctness of the geometric-center algorithms). *For $d \in \mathbb{N}$, $r \in \mathbb{R}_{>0}$, and $\varepsilon \in \mathbb{R}_{>0}$, the following statements hold for any execution that starts from an configuration in $Q^n \setminus \mathcal{S}_{\text{coinc}}$:*

- (i) *On the network \mathcal{S}_D , the law $\mathcal{CC}_{\text{VRN-CNTRD}}$ achieves the ε -distortion deployment task $\mathcal{T}_{\varepsilon\text{-distor-dply}}$. Moreover, any execution of the law $\mathcal{CC}_{\text{VRN-CNTRD}}$ monotonically optimizes the multicenter function $\mathcal{H}_{\text{dist}}$.*
- (ii) *On the network \mathcal{S}_D , any execution of the law $\mathcal{CC}_{\text{VRN-CRCMCNTR}}$ monotonically optimizes the multicenter function \mathcal{H}_{dc} .*
- (iii) *On the network \mathcal{S}_D , any execution of the law $\mathcal{CC}_{\text{VRN-NCNTR}}$ monotonically optimizes the multicenter function \mathcal{H}_{sp} .*

- (iv) On the network \mathcal{S}_{LD} , the law $\mathcal{CC}_{LMTD-VRN-NRML}$ achieves the ε -r-area deployment task $\mathcal{T}_{\varepsilon\text{-}r\text{-area-dply}}$. Moreover, any execution of the law $\mathcal{CC}_{LMTD-VRN-NRML}$ monotonically optimizes the multicenter function $\mathcal{H}_{\text{area}, \frac{r}{2}}$.
- (v) On the network \mathcal{S}_{LD} , the law $\mathcal{CC}_{LMTD-VRN-CNTRD}$ achieves the ε -r-distortion-area deployment task $\mathcal{T}_{\varepsilon\text{-r-distor-area-dply}}$. Moreover, any execution of $\mathcal{CC}_{LMTD-VRN-CNTRD}$ monotonically optimizes the multicenter function $\mathcal{H}_{\text{dist-area}, \frac{r}{2}}$.

The proof of this theorem is given in Section 5.5.1. The results on $\mathcal{CC}_{VRN-CNTRD}$ appeared originally in [Cortés et al. \(2004\)](#). Note that an execution of $\mathcal{CC}_{VRN-CNTRD}$ can be viewed as an alternating sequence of configuration of points and partitions of the space, with the properties that (i) each configuration of points corresponds to the set of centroid locations of the immediately preceding partition in the sequence, and (ii) each partition corresponds to the Voronoi partition determined by the immediately preceding configuration of points in the sequence. The monotonic behavior of $\mathcal{H}_{\text{dist}}$ now follows from Propositions 2.13 and 2.14. Similar interpretations can be given to all other laws. In particular, the monotonic behavior of \mathcal{H}_{dc} along executions of $\mathcal{CC}_{VRN-CRCMCNTR}$ can be established via Proposition 2.19, and the monotonic behavior of \mathcal{H}_{sp} along executions of $\mathcal{CC}_{VRN-NCNTR}$ can be established via Proposition 2.21. Continuous-time versions of these laws are studied by [Cortés and Bullo \(2005\)](#) via nonsmooth stability analysis, where the following convergence properties are established (recall the notion of active and passive nodes introduced in Sections 2.3.2 and 2.3.3): all active agents are guaranteed to asymptotically reach the circumcenter (resp., incenter) of their Voronoi region, whereas it is not known if the same conclusion holds for the passive agents. Depending on the polytope Q , there exist circumcenter and incenter Voronoi configurations where not all agents are active, and simulations show that in some cases the continuous-time versions of $\mathcal{CC}_{VRN-CRCMCNTR}$ and $\mathcal{CC}_{VRN-NCNTR}$ converge to them. It is an open research question to show that $\mathcal{CC}_{VRN-CRCMCNTR}$ and $\mathcal{CC}_{VRN-NCNTR}$ achieve the ε -disk-covering deployment task $\mathcal{T}_{\varepsilon\text{-dc-dply}}$ and the ε -sphere-packing deployment task $\mathcal{T}_{\varepsilon\text{-sp-dply}}$, respectively. Finally, the results on $\mathcal{CC}_{LMTD-VRN-NRML}$ and $\mathcal{CC}_{LMTD-VRN-CNTRD}$ appeared in [Cortés et al. \(2005\)](#).

Next, we analyze the time complexity of $\mathcal{CC}_{LMTD-VRN-CNTRD}$. We provide complete results only for the case $d = 1$ and uniform density. We assume that $\text{diam}(Q)$ is independent of n , r , and ε .

Theorem 5.6 (Time complexity of Lmtd-Vrn-cntrd law). *Assume that the robots evolve in a closed interval $Q \subset \mathbb{R}$, that is, $d = 1$, and assume that the density is uniform, that is, $\phi \equiv 1$. For $r \in \mathbb{R}_{>0}$ and $\varepsilon \in \mathbb{R}_{>0}$, on the network \mathcal{S}_{LD} , $\text{TC}(\mathcal{T}_{\varepsilon\text{-r-distor-area-dply}}, \mathcal{CC}_{LMTD-VRN-CNTRD}) \in O(n^3 \log(n\varepsilon^{-1}))$.*

The proof of this result is given in Section 5.5.2 following the treatment in Martínez et al. (2007).

Remark 5.7 (Congestion effects). Interestingly, Theorem 5.6 also holds if, motivated by wireless congestion considerations, we take the communication range r to be a monotone non-increasing function $r : \mathbb{N} \rightarrow]0, 2\pi[$ of the number of robotic agents n . •

5.3 SIMULATION RESULTS

In this section, we illustrate the execution of the various control and communication laws introduced in this chapter.

Geometric-center algorithms for expected-value optimization

The VRN-CNTRD, LMTD-VRN-NRML, and LMTD-VRN-CNTRD control and communication laws are implemented in Mathematica® as a library of routines and a main program running the simulation. The objective of a first routine is to compute the $\frac{r}{2}$ -limited Voronoi partition and parameterize each cell $V_{i,\frac{r}{2}}$, $i \in \{1, \dots, n\}$ in polar coordinates. The objective of a second routine is to compute the surface integrals on these sets and the line integrals on their boundaries via the numerical integration routine `NIntegrate`. We pay careful attention to numerical accuracy issues in the computation of the Voronoi diagram and in the integration.

Measuring displacements in meters, we consider the polygon Q determined by the vertices

$$\{(0,0), (2.125,0), (2.9325,1.5), (2.975,1.6), \\ (2.9325,1.7), (2.295,2.1), (0.85,2.3), (0.17,1.2)\}.$$

The diameter of Q is $\text{diam}(Q) \approx 3.378$. In all figures, the density function ϕ is the sum of four Gaussian functions of the form $11 \exp(6(-(x - x_{\text{center}})^2 - (y - y_{\text{center}})^2))$ and is represented by means of its contour plot. Darker-colored areas correspond to higher values of the density function. The four centers $(x_{\text{center}}, y_{\text{center}})$ of the Gaussian functions are the points $(2.15, 0.75)$, $(1.0, 0.25)$, $(0.725, 1.75)$ and $(0.25, 0.7)$, respectively. The area of the polygon is $A_\phi(Q) = 17.6352$.

We show evolutions of $(\mathcal{S}_D, \text{VRN-CNTRD})$ and $(\mathcal{S}_D, \text{VRN-CNTRD-DYNMCS})$ in Figures 5.2 and 5.3, respectively. One can verify that the final network configurations is a centroidal Voronoi configuration. In other words, the task $\mathcal{T}_{\epsilon\text{-distor-dply}}$ is achieved, as guaranteed by Theorem 5.5(i) for the VRN-

CNTRD ALGORITHM. For each evolution we depict the initial positions, the trajectories, and the final positions of all robots.

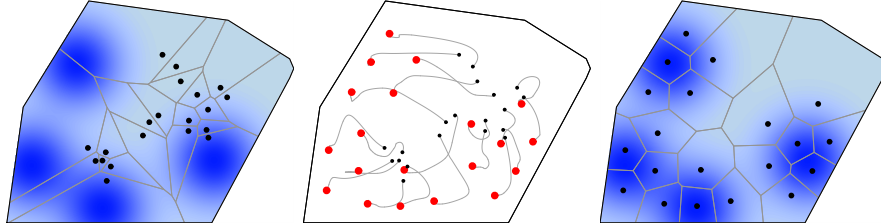


Figure 5.2 The evolution of $(\mathcal{S}_D, \text{VRN-CNTRD})$ with $n = 20$ robots. The left-hand (resp., right-hand) figure illustrates the initial (resp., final) locations and Voronoi partition. The central figure illustrates the evolution of the robots. After 13 seconds, the value of $\mathcal{H}_{\text{dist}}$ has monotonically increased to approximately -0.515 .

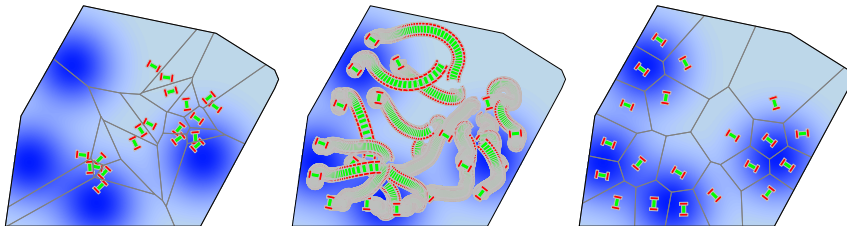


Figure 5.3 The evolution of $(\mathcal{S}_D, \text{VRN-CNTRD-DYNMCS})$ with $n = 20$ robots and with feedback gain $k_{\text{prop}} = 3.5$. The left-hand (resp., right-hand) figure illustrates the initial (resp., final) locations and Voronoi partition. The central figure illustrates the evolution of the robots. After 20 seconds, the value of $\mathcal{H}_{\text{dist}}$ has monotonically increased to approximately -0.555 .

We show an evolution of $(\mathcal{S}_{LD}, \text{LMTD-VRN-NRML})$ in Figure 5.4. One can verify that the final network configuration is an $\frac{r}{2}$ -limited area-centered Voronoi configuration. In other words, the task $\mathcal{T}_{\varepsilon-r\text{-area-dply}}$ is achieved, as guaranteed by Theorem 5.5(ii).

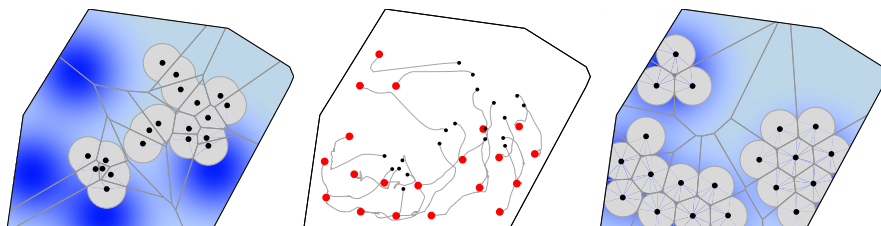


Figure 5.4 The evolution of $(\mathcal{S}_{LD}, \text{LMTD-VRN-NRML})$ with $n = 20$ robots and $r = 0.4$. The left-hand (resp., right-hand) figure illustrates the initial (respectively, final) locations and Voronoi partition. The central figure illustrates the evolution of the robots. The $\frac{r}{2}$ -limited Voronoi cell of each robot is plotted in light gray. After 36 seconds, the value of $\mathcal{H}_{\text{area}, \frac{r}{2}}$ has monotonically increased to approximately 14.141.

We show an evolution of $(\mathcal{S}_{LD}, \text{LMTD-VRN-CNTRD})$ in Figure 5.5. One can verify that the final network configuration is a $\frac{r}{2}$ -limited centroidal Voronoi configuration. In other words, the task $\mathcal{T}_{\varepsilon-r\text{-distor-area-dply}}$ is achieved, as guaranteed by Theorem 5.5(iii).

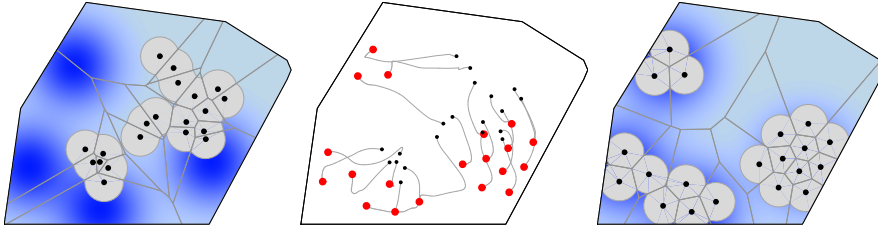


Figure 5.5 The evolution of $(\mathcal{S}_{LD}, \text{LMTD-VRN-CNTRD})$ with $n = 20$ robots and $r = 0.4$. The left-hand (resp., right-hand) figure illustrates the initial (resp., final) locations and Voronoi partition. The central figure illustrates the evolution of the robots. The $\frac{r}{2}$ -limited Voronoi cell of each robot is plotted in light gray. After 90 seconds, the value of $\mathcal{H}_{\text{dist-area}, \frac{r}{2}}$ reaches approximately -0.386 .

We show an evolution of $(\mathcal{S}_{LD}, \text{RNG-VRN-CNTRD})$ in Figure 5.6. One can verify that the final network configuration corresponds to a critical point of the mixed distortion-area multicenter function $\mathcal{H}_{\text{dist-area}, \frac{r}{2}, b}$, with $b = -\text{diam}(Q)^2$ (see Exercise E.4).

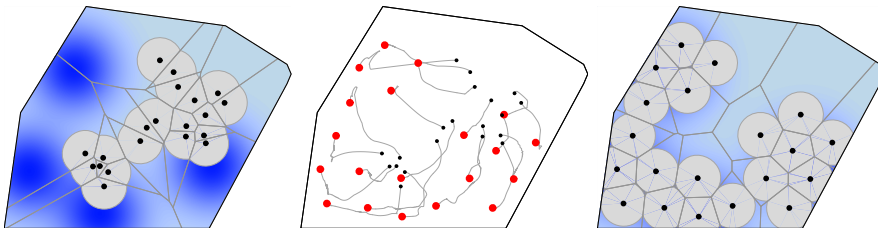


Figure 5.6 The evolution of $(\mathcal{S}_{LD}, \text{RNG-VRN-CNTRD})$ with $n = 20$ robots and $r = 0.47$. The left-hand (resp., right-hand) figure illustrates the initial (respectively, final) locations and Voronoi partition. The central figure illustrates the evolution of the robots. The $\frac{r}{2}$ -limited Voronoi cell of each robot is plotted in light gray. After 13 seconds, the value of $\mathcal{H}_{\text{dist-area}, \frac{r}{2}, b}$, with $b = -\text{diam}(Q)^2$, is approximately -4.794 .

As discussed in Remark 5.4, RNG-VRN-CNTRD can be understood as a range-limited implementation of VRN-CNTRD in a network of robots with range-limited interactions. Let us briefly compare the evolutions depicted in Figures 5.2 and 5.6. According to Proposition 2.17, we compute

$$\beta = \frac{\frac{r}{2}}{\text{diam } Q} \approx 0.06957.$$

From the constant-factor approximation (2.3.7), the absolute error is guaranteed to be less than or equal to $(\beta^2 - 1)\mathcal{H}_{\text{dist-area}, \frac{r}{2}, b}(P_{\text{final}}) \approx 4.77$, where P_{final} denotes the final configuration in Figure 5.6. The percentage error in the value of the multicenter function $\mathcal{H}_{\text{dist}}$ between the final configuration of the evolution in Figure 5.2 and the final configuration of the evolution in Figure 5.6 is approximately equal to 3.277%. As expected, one can verify in simulations that the percentage error of the performance of the range-limited implementation improves with higher values of the ratio $\frac{r}{\text{diam } Q}$.

Geometric-center algorithms for disk-covering and sphere-packing

The VRN-CRCMCNTR and VRN-NCNTR control and communication laws are implemented in Mathematica® as a single centralized program running the simulation. We compute the bounded Voronoi diagram of a collection of points using the package ComputationalGeometry. We compute the circumcenter of a polygon via the algorithm in [Skyum \(1991\)](#) and the incenter set via the LinearProgramming solver in Mathematica®.

Measuring displacements in meters, we consider the polygon determined by the vertices

$$\{(0, 0), (2.5, 0), (3.45, 1.5), (3.5, 1.6), \\ (3.45, 1.7), (2.7, 2.1), (1.0, 2.4), (0.2, 1.2)\}.$$

We show an evolution of $(\mathcal{S}_D, \text{VRN-CRCMCNTR})$ in Figure 5.7. One can verify that in the final configuration all robots are at the circumcenter of their own Voronoi cell. In other words, the task $\mathcal{T}_{\varepsilon-\text{dc-dply}}$ is achieved by this evolution. As stated in Section 5.2.3, it is an open research question to show that this fact holds in general for $\mathcal{CC}_{\text{VRN-CRCMCNTR}}$. [Cortés and Bullo \(2005\)](#) prove a similar result for a continuous-time implementation of this law.

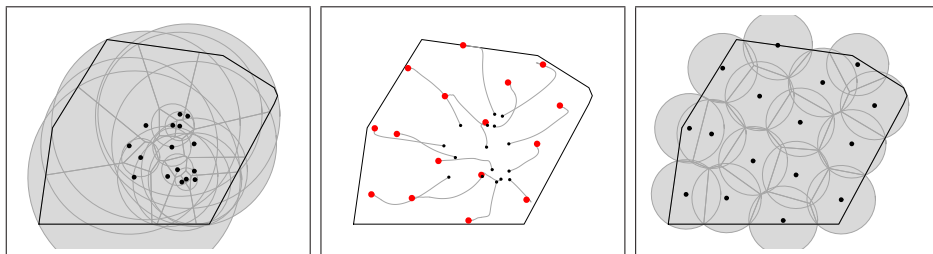


Figure 5.7 The evolution of $(\mathcal{S}_D, \text{VRN-CRCMCNTR})$ with $n = 16$ robots. The left-hand (resp., right-hand) figure illustrates the initial (resp., final) locations and Voronoi partition. The central figure illustrates the evolution of the robots. After 20 seconds, the value of \mathcal{H}_{dc} has monotonically decreased to approximately 0.43273 meters.

We show an evolution of $(\mathcal{S}_D, \text{VRN-NCNTR})$ in Figure 5.8. One can verify that in the final configuration all robots are at the incenter of their own Voronoi cell. In other words, the task $\mathcal{T}_{\varepsilon\text{-sp-dply}}$ is achieved by this evolution. As stated in Section 5.2.3, it is an open research question to show that this fact holds in general for $\mathcal{CC}_{\text{VRN-NCNTR}}$. [Cortés and Bullo \(2005\)](#) prove a similar result for a continuous-time implementation of this law.

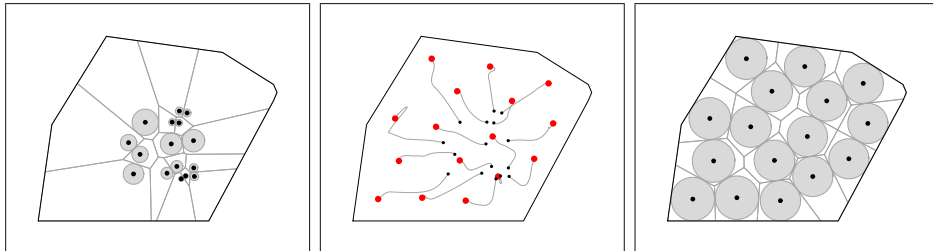


Figure 5.8 The evolution of $(\mathcal{S}_D, \text{VRN-NCNTR})$ with $n = 16$ robots. The left-hand (resp., right-hand) figure illustrates the initial (resp., final) locations and Voronoi partition. The central figure illustrates the evolution of the robots. After 20 seconds, the value of \mathcal{H}_{sp} has monotonically increased to approximately 0.2498 meters.

5.4 NOTES

The deployment problem studied in this chapter is related to the literature on facility location ([Drezner, 1995](#); [Okabe et al., 2000](#); [Du et al., 1999](#)) and geometric optimization ([Agarwal and Sharir, 1998](#); [Boltyanski et al., 1999](#)) (see also Section 2.4). These disciplines study spatial resource allocation problems and play an important role in quantization theory, mesh and grid optimization methods, clustering analysis, data compression, and statistical pattern recognition. Indeed, our algorithms are closely related to some early work by [Lloyd \(1982\)](#) on “centering and partitioning” algorithms for optimal quantizer design.

Dispersion laws have been traditionally studied in behavior control (see, e.g., ([Arkin, 1998](#); [Schultz and Parker, 2002](#); [Balch and Parker, 2002](#))). Deployment algorithms that make use of potential field methods are proposed by [Payton et al. \(2001\)](#) and [Howard et al. \(2002\)](#). Other works include ([Bulusu et al., 2001](#)) on adaptive beacon placement for localization, [Poduri and Sukhatme \(2004\)](#) on network deployments that satisfy a pre-specified constraint in the number of neighbors of each robot, [Arsie et al. \(2009\)](#) on sensor-based deployment strategies that minimize the expected service time for newly appearing target points, and [Hussein and Stipanović \(2007\)](#) on dynamically surveying a known environment.

Deployment algorithms for coverage control are a subject of active re-

search. Among the most recent works, Martínez (2009) and Schwager et al. (2009) consider coverage problems where the density function is unknown, Lekien and Leonard (2009) propose centralized laws for non-uniform coverage using cartograms, de Silva and Ghrist (2007) study static coverage problems with minimal assumptions on the capabilities of individual sensors using algebraic topology, Kwok and Martínez (2009) propose distributed deployment strategies for energy-constrained networks, Laventall and Cortés (2009) design distributed algorithms for networks of robots whose sensors have range-limited wedge-shaped footprints, Gao et al. (2008) consider discrete coverage problems, Schwager et al. (2008) consider joint exploration and deployment problems, and Zhong and Cassandras (2008), Pimenta et al. (2008), and Caicedo-Núñez and Žefran (2008) deal with centroidal Voronoi tessellations in nonconvex environments. Graham and Cortés (2009) study the optimality of circumcenter and incenter Voronoi configurations for the estimation of stochastic spatial fields. Susca et al. (2009) consider some planar interpolation problems. Finally, Cortés (2008); Pavone et al. (2008) consider equitable partitioning policies in which the workspace is divided into subregions of equal area and their application to vehicle routing problems.

Deployment problems play a relevant role in other coordination tasks, such as surveillance, search and rescue, and exploration and map building of unknown environments. Choset (2001) considers sweep coverage problems, where one or more robots equipped with limited footprint sensors have to visit all points in the environment. In Simmons et al. (2000), deployment locations for a network of heterogeneous robots are user-specified after an initial map of the unknown environment has been built. Gupta et al. (2006) consider a combined sensor coverage and selection problem.

Deployment of robotic agents with visibility sensors has been studied under a variety of assumptions. When the environment is known *a priori*, the problem can be cast as the classical Art Gallery Problem (Chvátal, 1975) from computational geometry, where one is interested in achieving complete visibility with the minimum number of agents possible. The Art Gallery Problem is computationally hard (Lee and Lin, 1986; Eidenbenz et al., 2001) and the best-known approximation algorithms yield solutions within a logarithmic factor of the optimum number of agents (Ghosh, 1987; Efrat and Har-Peled, 2006). Pinciu (2003) and Hernández-Peña (1994) study the problem of achieving full visibility while guaranteeing that the final network configuration will have a connected visibility graph. Recent works on multi-robot exploration of unknown environments include (Batalin and Sukhatme, 2004), Burgard et al. (2005), and Howard et al. (2006). Topological exploration of graph-like environments by single and multiple robots is studied in Rekleitis et al. (2001), Fraigniaud et al. (2004), and Dynia et al. (2006).

A simple one-step strategy for visibility deployment, without the need for synchronization, achieving the worst-case optimal bounds in terms of the number of robots required, and under limited communication, is presented in Ganguli et al. (2007).

5.5 PROOFS

This section gathers the proofs of the main results presented in the chapter.

5.5.1 Proof of Theorem 5.5

Proof. Let $P_0 = (p^{[1]}(0), \dots, p^{[n]}(0)) \in Q^n \setminus \mathcal{S}_{\text{coinc}}$ denote the initial condition. The proof strategy for all five facts is similar and is based on the application of the LaSalle Invariance Principle with Lyapunov function given by an appropriate multicenter function. In other words, we need to establish the monotonic behavior of the certain multicenter functions along the executions of the control and communication laws and we need to characterize certain invariant sets using geometric properties of the multicenter functions. Additionally, in order to apply the LaSalle Invariance Principle, we need to work with the set $Q^n \setminus \mathcal{S}_{\text{coinc}}$ which is not closed and, therefore, we rely upon the extension of Theorem 1.19 given in Exercise E1.8(ii).

In what follows, we discuss in detail the proof of fact (i) regarding the control and communication law $\mathcal{CC}_{\text{VRN-CNTRD}}$ for the network \mathcal{S}_D . We leave it to the reader to fill out some of the proof details for the other laws.

Fact (i). First, note that, starting from a configuration in $Q^n \setminus \mathcal{S}_{\text{coinc}}$, one step of the law $\mathcal{CC}_{\text{VRN-CNTRD}}$ leads the network to another configuration in $Q^n \setminus \mathcal{S}_{\text{coinc}}$. Therefore, it is convenient to let $f_{\text{VRN-CNTRD}} : Q^n \setminus \mathcal{S}_{\text{coinc}} \rightarrow Q^n \setminus \mathcal{S}_{\text{coinc}}$ denote the map induced by the execution of one step of the control and communication law $\mathcal{CC}_{\text{VRN-CNTRD}}$.

To apply Theorem 1.19, we work with the set $W = Q^n \setminus \mathcal{S}_{\text{coinc}}$. Clearly, this set is positively invariant for $f_{\text{VRN-CNTRD}}$ and it is bounded. Therefore, assumptions (i) and (iii) of Theorem 1.19 are satisfied, except for the closedness of W . Next, we show that executions of the law $\mathcal{CC}_{\text{VRN-CNTRD}}$ monotonically optimize the function $\mathcal{H}_{\text{dist}}$. Using the extension of the multicenter function defined over the set of points and partitions of Q , we deduce from Proposition 2.13 that, for $P \in Q^n \setminus \mathcal{S}_{\text{coinc}}$,

$$\begin{aligned}\mathcal{H}_{\text{dist}}(f_{\text{VRN-CNTRD}}(P)) &= \mathcal{H}_{\text{dist}}(f_{\text{VRN-CNTRD}}(P), \mathcal{V}(f_{\text{VRN-CNTRD}}(P))) \\ &\geq \mathcal{H}_{\text{dist}}(f_{\text{VRN-CNTRD}}(P), \mathcal{V}(P)).\end{aligned}$$

The application of Proposition 2.14 yields

$$\mathcal{H}_{\text{dist}}(f_{\text{VRN-CNTRD}}(P), \mathcal{V}(P)) \geq \mathcal{H}_{\text{dist}}(P, \mathcal{V}(P)),$$

and, therefore, $\mathcal{H}_{\text{dist}}(f_{\text{VRN-CNTRD}}(P)) \geq \mathcal{H}_{\text{dist}}(P)$. Additionally, recall from Proposition 2.14, that, for $P \in Q^n \setminus \mathcal{S}_{\text{coinc}}$, the inequality is strict unless $f_{\text{VRN-CNTRD}}(P) = P$. This discussion establishes assumption (ii) of Theorem 1.19. The continuity of the map $f_{\text{VRN-CNTRD}} : Q^n \setminus \mathcal{S}_{\text{coinc}} \rightarrow Q^n \setminus \mathcal{S}_{\text{coinc}}$, is a consequence of the following two facts. First, one can verify that each Voronoi cell is a convex set whose boundary is a piecewise continuously differentiable function of the positions of the robots. Second, given a convex set whose boundary depends upon a parameter in a piecewise continuously differentiable fashion, Proposition 2.23 guarantees that the centroid of that set is a continuously differentiable function of the parameter. This discussion and the continuity of $\mathcal{H}_{\text{dist}}$ establishes assumption (iv) of Theorem 1.19.

In the following, we consider an evolution $\gamma : \mathbb{Z}_{\geq 0} \rightarrow Q^n \setminus \mathcal{S}_{\text{coinc}}$ of $f_{\text{VRN-CNTRD}}$ and we prove that no point in $\mathcal{S}_{\text{coinc}}$ may be an accumulation point of γ . By contradiction, we assume that $P = (p_1, \dots, p_n) \in \mathcal{S}_{\text{coinc}}$ is an accumulation point for γ . Our first claim is that there exists a sequence of increasing times $\{\ell_k \mid k \in \mathbb{N}\}$ and unit-length vectors $u_{ij} \in \mathbb{R}^d$, for $i, j \in \{1, \dots, n\}$, such that $\gamma(\ell_k) \rightarrow P$ and simultaneously $\text{vers}(\gamma_i(\ell_k) - \gamma_j(\ell_k)) \rightarrow u_{ij}$ as $k \rightarrow \infty$. Here, the versor operator $\text{vers} : \mathbb{R}^d \rightarrow \mathbb{R}^d$ is defined by $\text{vers}(\mathbf{0}_d) = \mathbf{0}_d$ and $\text{vers}(v) = v/\|v\|_2$ for $v \neq \mathbf{0}_d$. This first claim is true because P is an accumulation point and because the sequences $\ell \mapsto \text{vers}(\gamma_i(\ell) - \gamma_j(\ell))$ take value in a compact set. Our second claim is that, as $k \rightarrow \infty$, the sequence of partitions $\mathcal{V}(\gamma(\ell_k))$ has a limiting partition, say $\{V_1^\infty, \dots, V_n^\infty\}$. This second claim is true because, for each pair of robots i and j converging to the same position $p_i = p_j$, the bisector of the segment connecting them admits a limit that is equal to the line through the point $p_i = p_j$ and perpendicular to the unit-length vector u_{ij} . Therefore, each of the edges of each of the polygons $\mathcal{V}(\gamma(\ell_k))$ has a limit for $k \rightarrow \infty$. Finally, note that each polygon V_i^∞ has a positive measure.

We know that $\ell \mapsto \mathcal{H}_{\text{dist}}(\gamma(\ell))$ is monotonically non-increasing and lower-bounded. Therefore, we must have that

$$\lim_{\ell \rightarrow \infty} (\mathcal{H}_{\text{dist}}(\gamma(\ell)) - \mathcal{H}_{\text{dist}}(\gamma(\ell + 1))) = 0. \quad (5.5.1)$$

Define the short-hand $W_{k,1} = V_1(\gamma(\ell_k))$, and compute

$$\begin{aligned} & \lim_{k \rightarrow \infty} \left(\mathcal{H}_{\text{dist}}(\gamma(\ell_k)) - \mathcal{H}_{\text{dist}}(\gamma(\ell_k + 1)) \right) \\ & \geq \lim_{k \rightarrow \infty} \left(\int_{W_{k,1}} \|q - \gamma_1(\ell_k)\|_2^2 \phi(q) dq - \int_{W_{k,1}} \|q - \text{CM}_\phi(W_{k,1})\|_2^2 \phi(q) dq \right) \end{aligned} \quad (5.5.2)$$

$$= \int_{V_1^\infty} \|q - p_1\|_2^2 \phi(q) dq - \int_{V_1^\infty} \|q - \text{CM}_\phi(V_1^\infty)\|_2^2 \phi(q) dq \quad (5.5.3)$$

$$= A_\phi(V_1^\infty) \|p_1 - \text{CM}_\phi(V_1^\infty)\|_2, \quad (5.5.4)$$

where inequality (5.5.2) follows from Proposition 2.14, equality (5.5.3) follows from the definition of the limiting partition $\{V_1^\infty, \dots, V_n^\infty\}$, and equation (5.5.4) follows from the Parallel Axis Theorem. Now, the quantity $A_\phi(V_1^\infty)$ is strictly positive, as mentioned above, and the quantity $\|p_1 - \text{CM}_\phi(V_1^\infty)\|_2$ is strictly positive because $p_1 \in \partial V_1^\infty$ and $\text{CM}_\phi(V_1^\infty)$ belongs to the interior of V_1^∞ by Exercise (E2.2). The fact that the last limit is lower bounded by a positive is a contradiction with equation (5.5.1). Therefore, we now know that no point in $\mathcal{S}_{\text{coinc}}$ may be an accumulation point of γ .

Finally, we are now ready to apply the LaSalle Invariance Principle as stated in Exercise E1.8(ii) and deduce that the execution of $\mathcal{CC}_{\text{VRN-CNTRD}}$ starting from $P_0 \in Q^n \setminus \mathcal{S}_{\text{coinc}}$ tends to the largest positively invariant set S contained in

$$\{P \in Q^n \mid \mathcal{H}_{\text{dist}}(f_{\text{VRN-CNTRD}}(P)) = \mathcal{H}_{\text{dist}}(P)\}.$$

The set S is precisely the set of centroidal Voronoi configurations. This result is a consequence of the fact that $\mathcal{H}_{\text{dist}}(f_{\text{VRN-CNTRD}}(P)) = \mathcal{H}_{\text{dist}}(P)$ implies that $f_{\text{VRN-CNTRD}}(P) = P$, that is, P is a centroidal Voronoi configuration.

Facts (ii) and (iii). The proofs of these facts run parallel to the proof of fact (i). Propositions 2.19 and 2.21 are key in establishing the monotonic evolution of \mathcal{H}_{dc} and \mathcal{H}_{sp} , respectively.

Fact (iv). Let $f_{\text{LMTD-VRN-NRML}} : Q^n \setminus \mathcal{S}_{\text{coinc}} \rightarrow Q^n \setminus \mathcal{S}_{\text{coinc}}$ denote the map induced by the execution of one step of the law $\mathcal{CC}_{\text{LMTD-VRN-NRML}}$. Let us show that executions of $\mathcal{CC}_{\text{LMTD-VRN-NRML}}$ monotonically optimize the function $\mathcal{H}_{\text{area}, \frac{r}{2}}$. Using the extension of the multicenter function defined over the set of points and partitions of Q , we deduce from Proposition 2.13 that, for $P \in Q^n \setminus \mathcal{S}_{\text{coinc}}$,

$$\begin{aligned} & \mathcal{H}_{\text{area}, \frac{r}{2}}(f_{\text{LMTD-VRN-NRML}}(P)) \\ & = \mathcal{H}_{\text{area}, \frac{r}{2}}(f_{\text{LMTD-VRN-NRML}}(P), \mathcal{V}(f_{\text{LMTD-VRN-NRML}}(P))) \\ & \geq \mathcal{H}_{\text{area}, \frac{r}{2}}(f_{\text{LMTD-VRN-NRML}}(P), \mathcal{V}(P)). \end{aligned}$$

The line search procedure for each robot embedded in the definition of the control function of $\mathcal{CC}_{\text{LMTD-VRN-NRML}}$ ensures that

$$\mathcal{H}_{\text{area}, \frac{r}{2}}(f_{\text{LMTD-VRN-NRML}}(P), \mathcal{V}(P)) \geq \mathcal{H}_{\text{area}, \frac{r}{2}}(P, \mathcal{V}(P)),$$

and hence, $\mathcal{H}_{\text{area}, \frac{r}{2}}(f_{\text{LMTD-VRN-NRML}}(P)) \geq \mathcal{H}_{\text{area}, \frac{r}{2}}(P)$. Note that the inequality is strict unless $f_{\text{LMTD-VRN-NRML}}(P) = P$. We leave it to the interested reader to prove, similarly to what we did for fact (i), that the map $f_{\text{LMTD-VRN-NRML}}$ is continuous and that no point in $\mathcal{S}_{\text{coinc}}$ may be an accumulation point of any trajectory of $f_{\text{LMTD-VRN-NRML}}$. Finally, the application of the LaSalle Invariance Principle as in the proof of fact (i) leads us to the result stated in fact (iv).

Fact (v). The proof of this fact runs parallel to the proofs of facts (i) and (iv). Propositions 2.13 and 2.15 are key in establishing the monotonic evolution of the cost function $\mathcal{H}_{\text{dist-area}, \frac{r}{2}}$. ■

5.5.2 Proof of Theorem 5.6

Proof. For $d = 1$, Q is a compact interval on \mathbb{R} —say $Q = [q_-, q_+]$. We start with a brief discussion about connectivity. In the r -limited Delaunay graph, two agents that are at most at a distance r from each other are neighbors if and only if there are no other agents between them. Additionally, we claim that if agents i and j are neighbors, then $|\text{CM}_\phi(V^{[i]}) - \text{CM}_\phi(V^{[j]})| \leq r$, where $V^{[i]}$ denotes the set defined by the control function ctl when evaluated by agent i . To show this fact, let us assume without loss of generality that $p_-^{[i]} \leq p_-^{[j]}$. Let us consider the case where the agents have neighbors on both sides (the other cases can be treated analogously). Let $p_-^{[i]}$ (resp., $p_+^{[i]}$) denote the position of the neighbor of agent i to the left (resp., of agent j to the right). Now,

$$\begin{aligned} \text{CM}_\phi(V^{[i]}) &= \frac{1}{4}(p_-^{[i]} + 2p^{[i]} + p_+^{[i]}), \\ \text{CM}_\phi(V^{[j]}) &= \frac{1}{4}(p_-^{[j]} + 2p^{[j]} + p_+^{[j]}), \end{aligned}$$

where we have used the fact that $\phi \equiv 1$. Therefore,

$$|\text{CM}_\phi(V^{[i]}) - \text{CM}_\phi(V^{[j]})| \leq \frac{1}{4}(|p_-^{[i]} - p_-^{[j]}| + 2|p^{[i]} - p^{[j]}| + |p_+^{[i]} - p_+^{[j]}|) \leq r.$$

This implies that agents i and j belong to the same connected component of the r -limited Delaunay graph at the next time step.

Next, let us consider the case when $\mathcal{G}_{\text{LD}}(r)$ is connected at the initial network configuration $P_0 = (p^{[1]}(0), \dots, p^{[n]}(0))$. Without loss of generality,

assume that the agents are ordered from left to right according to their unique identifier, that is, $p^{[1]}(0) \leq \dots \leq p^{[n]}(0)$. We distinguish three cases depending on the proximity of the leftmost and rightmost agents 1 and n , respectively, to the boundary of the environment: in case **(a)** both agents are within a distance $\frac{r}{2}$ of ∂Q ; in case **(b)**, neither of the two is within a distance $\frac{r}{2}$ of ∂Q ; and in case **(c)** only one of the agents is within a distance $\frac{r}{2}$ of ∂Q . Here is an important observation: from one time instant to the next, the network configuration can fall into any of the cases described above. However, because of the discussion on connectivity, transitions can only occur from case **(b)** to either case **(a)** or case **(c)**; and from case **(c)** to case **(a)**. As we show below, for each of these cases, the network evolution under $\mathcal{CC}_{\text{VRN-CNTRD}}$ can be described as a discrete-time linear dynamical system which respects agents' ordering.

Let us consider case **(a)**. In this case, we have

$$\begin{aligned} p^{[1]}(\ell + 1) &= \frac{1}{4}(p^{[1]}(\ell) + p^{[2]}(\ell)) + \frac{1}{2}q_-, \\ p^{[2]}(\ell + 1) &= \frac{1}{4}(p^{[1]}(\ell) + 2p^{[2]}(\ell) + p^{[3]}(\ell)), \\ &\vdots \\ p^{[n-1]}(\ell + 1) &= \frac{1}{4}(p^{[n-2]}(\ell) + 2p^{[n-1]}(\ell) + p^{[n]}(\ell)), \\ p^{[n]}(\ell + 1) &= \frac{1}{4}(p^{[n-1]}(\ell) + p^{[n]}(\ell)) + \frac{1}{2}q_+. \end{aligned}$$

Equivalently, we can write $P(\ell + 1) = A_{(\mathbf{a})} \cdot P(\ell) + b_{(\mathbf{a})}$, where the matrix $A_{(\mathbf{a})} \in \mathbb{R}^{n \times n}$ and the vector $b_{(\mathbf{a})} \in \mathbb{R}^n$ are given by

$$A_{(\mathbf{a})} = \begin{bmatrix} \frac{1}{4} & \frac{1}{4} & 0 & \dots & \dots & 0 \\ \frac{1}{4} & \frac{1}{2} & \frac{1}{4} & \dots & \dots & 0 \\ 0 & \frac{1}{4} & \frac{1}{2} & \frac{1}{4} & \dots & 0 \\ \vdots & \ddots & \ddots & \ddots & \ddots & \vdots \\ 0 & \dots & \dots & \frac{1}{4} & \frac{1}{2} & \frac{1}{4} \\ 0 & \dots & \dots & 0 & \frac{1}{4} & \frac{1}{4} \end{bmatrix}, \quad b_{(\mathbf{a})} = \begin{bmatrix} \frac{1}{2}q_- \\ 0 \\ \vdots \\ 0 \\ \frac{1}{2}q_+ \end{bmatrix}.$$

Note that the only equilibrium network configuration P_* respecting the ordering of the agents is given by

$$p_*^{[i]} = q_- + \frac{1}{2n}(1 + 2(i - 1))(q_+ - q_-), \quad i \in \{1, \dots, n\},$$

and note that this is a $\frac{r}{2}$ -centroidal Voronoi configuration (under the assumption of case **(a)**). We can therefore write $(P(\ell + 1) - P_*) = A_{(\mathbf{a})}(P(\ell) - P_*)$. Now, note that $A_{(\mathbf{a})} = \text{ATrid}_n^-(\frac{1}{4}, \frac{1}{2})$. Theorem 1.80(ii) implies that $\lim_{\ell \rightarrow +\infty} (P(\ell) - P_*) = \mathbf{0}_n$, and that the maximum time required for $\|P(\ell) -$

$\|P_*\|_2 \leq \varepsilon \|P_0 - P_*\|_2$ (over all initial conditions in \mathbb{R}^n) is $\Theta(n^2 \log \varepsilon^{-1})$. It is not obvious, but it can be verified, that the initial condition providing the lower bound in the time complexity estimate does indeed have the property of respecting the agents' ordering; this fact holds for all three possible cases **(a)**, **(b)**, and **(c)**.

Case **(b)** can be treated in the same way. The network evolution now takes the form $P(\ell + 1) = A_{(b)} \cdot P(\ell) + b_{(b)}$, where the matrix $A_{(b)} \in \mathbb{R}^{n \times n}$ and the vector $b_{(b)} \in \mathbb{R}^n$ are given by

$$A_{(b)} = \begin{bmatrix} \frac{3}{4} & \frac{1}{4} & 0 & \dots & \dots & 0 \\ \frac{1}{4} & \frac{1}{4} & \frac{1}{4} & \dots & \dots & 0 \\ \frac{1}{4} & \frac{1}{2} & \frac{1}{4} & \frac{1}{4} & \dots & 0 \\ 0 & \frac{1}{4} & \frac{1}{2} & \frac{1}{4} & \dots & 0 \\ \vdots & \ddots & \ddots & \ddots & \ddots & \vdots \\ 0 & \dots & \dots & \frac{1}{4} & \frac{1}{2} & \frac{1}{3} \\ 0 & \dots & \dots & 0 & \frac{1}{4} & \frac{3}{4} \end{bmatrix}, \quad b_{(b)} = \begin{bmatrix} -\frac{1}{4}r \\ 0 \\ \vdots \\ 0 \\ \frac{1}{4}r \end{bmatrix}.$$

In this case, a (non-unique) equilibrium network configuration respecting the ordering of the agents is of the form

$$p_*^{[i]} = ir - \frac{1+n}{2}r, \quad i \in \{1, \dots, n\}.$$

Note that this is a $\frac{r}{2}$ -centroidal Voronoi configuration (under the assumption of case **(b)**). We can therefore write $(P(\ell + 1) - P_*) = A_{(b)}(P(\ell) - P_*)$. Now, observe that $A_{(b)} = \text{ATrid}_n^+(\frac{1}{4}, \frac{1}{2})$. We compute that $P_{\text{ave}} = \frac{1}{n}\mathbf{1}_n^T(P_0 - P_*) = \frac{1}{n}\mathbf{1}_n^T P_0$. With this calculation, Theorem 1.80(i) implies that $\lim_{\ell \rightarrow +\infty} (P(\ell) - P_* - P_{\text{ave}}\mathbf{1}_n) = \mathbf{0}_n$, and that the maximum time required for $\|P(\ell) - P_* - P_{\text{ave}}\mathbf{1}_n\|_2 \leq \varepsilon \|P_0 - P_* - P_{\text{ave}}\mathbf{1}_n\|_2$ (over all initial conditions in \mathbb{R}^n) is $\Theta(n^2 \log \varepsilon^{-1})$.

Case **(c)** needs to be handled differently. Without loss of generality, assume that agent 1 is within distance $\frac{r}{2}$ of ∂Q and agent n is not (the other case is treated analogously). Then, the network evolution now takes the form $P(\ell + 1) = A_{(c)} \cdot P(\ell) + b_{(c)}$, where the matrix $A_{(c)} \in \mathbb{R}^{n \times n}$ and the vector $b_{(c)} \in \mathbb{R}^n$ are given by

$$A_{(c)} = \begin{bmatrix} \frac{1}{4} & \frac{1}{4} & 0 & \dots & \dots & 0 \\ \frac{1}{4} & \frac{1}{2} & \frac{1}{4} & \dots & \dots & 0 \\ \frac{1}{4} & \frac{1}{2} & \frac{1}{4} & \frac{1}{4} & \dots & 0 \\ 0 & \frac{1}{4} & \frac{1}{2} & \frac{1}{4} & \dots & 0 \\ \vdots & \ddots & \ddots & \ddots & \ddots & \vdots \\ 0 & \dots & \dots & \frac{1}{4} & \frac{1}{2} & \frac{1}{4} \\ 0 & \dots & \dots & 0 & \frac{1}{4} & \frac{3}{4} \end{bmatrix}, \quad b_{(c)} = \begin{bmatrix} \frac{1}{2}q \\ 0 \\ \vdots \\ 0 \\ \frac{1}{4}r \end{bmatrix}.$$

Note that the only equilibrium network configuration P_* respecting the or-

dering of the agents is given by

$$p_*^{[i]} = q_- + \frac{1}{2}(2i - 1)r, \quad i \in \{1, \dots, n\},$$

and note that this is a $\frac{r}{2}$ -centroidal Voronoi configuration (under the assumption of case **(c)**). In order to analyze $A_{(c)}$, we recast the n -dimensional discrete-time dynamical system as a $2n$ -dimensional one. To do this, we define a $2n$ -dimensional vector y by

$$y^{[i]} = p^{[i]}, \quad i \in \{1, \dots, n\}, \quad \text{and} \quad y^{[n+i]} = p^{[n-i+1]}, \quad i \in \{1, \dots, n\}. \quad (5.5.5)$$

Now, one can see that the network evolution can be alternatively described in the variables $(y^{[1]}, \dots, y^{[2n]})$ as a linear dynamical system determined by the $2n \times 2n$ matrix $\text{ATrid}_{2n}^-(\frac{1}{4}, \frac{1}{2})$. Using Theorem 1.80(ii), and exploiting the chain of equalities (5.5.5), it is possible to infer that, in case **(c)**, the maximum time required for $\|P(\ell) - P_*\|_2 \leq \varepsilon \|P_0 - P_*\|_2$ (over all initial conditions in \mathbb{R}^n) is $\Theta(n^2 \log \varepsilon^{-1})$.

In summary, for all three cases **(a)**, **(b)**, and **(c)**, our calculations show that, in time $O(n^2 \log \varepsilon^{-1})$, the error 2-norm satisfies the contraction inequality $\|P(\ell) - P_*\|_2 \leq \varepsilon \|P_0 - P_*\|_2$. We convert this inequality on 2-norms into an appropriate inequality on ∞ -norms as follows. Note that $\|P_0 - P_*\|_\infty = \max_{i \in \{1, \dots, n\}} |p^{[i]}(0) - p_*^{[i]}| \leq (q_+ - q_-)$. For ℓ of order $n^2 \log \eta^{-1}$, we have that

$$\begin{aligned} \|P(\ell) - P_*\|_\infty &\leq \|P(\ell) - P_*\|_2 \leq \eta \|P_0 - P_*\|_2 \\ &\leq \eta \sqrt{n} \|P_0 - P_*\|_\infty \leq \eta \sqrt{n} (q_+ - q_-). \end{aligned}$$

This means that ε - r -deployment is achieved for $\eta \sqrt{n} (q_+ - q_-) = \varepsilon$, that is, in time $O(n^2 \log \eta^{-1}) = O(n^2 \log(n\varepsilon^{-1}))$.

Up to here, we have proved that if the graph $\mathcal{G}_{\text{LD}}(r)$ is connected at P_0 , then $\text{TC}(\mathcal{T}_{\varepsilon-r\text{-dply}}, \mathcal{CC}_{\text{VRN-CNTRD}}, P_0) \in O(n^2 \log(n\varepsilon^{-1}))$. If $\mathcal{G}_{\text{LD}}(r)$ is not connected at P_0 , note that along the network evolution there can only be a finite number of time instants, at most $n - 1$ where a merging of two connected components occurs. Therefore, the time complexity is at most $O(n^3 \log(n\varepsilon^{-1}))$, as claimed. \blacksquare

5.6 EXERCISES

- E5.1 **(The Vrn-crcmcntr law is not positively invariant on $Q^n \setminus \mathcal{S}_{\text{coinc}}$).** Consider the network \mathcal{S}_D composed by 2 robots evolving in the convex polygon depicted in Figure E5.1. Describe the evolution of the network starting from the configuration depicted in Figure E5.1 and discuss its implication on the positive invariance of the set $Q^2 \setminus \mathcal{S}_{\text{coinc}}$ with respect to $\mathcal{CC}_{\text{VRN-CRCMCNTR}}$.

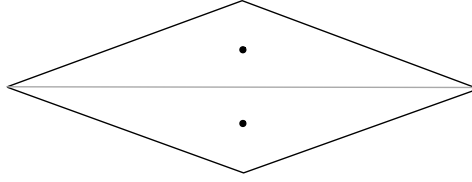


Figure E5.1 Convex polygon for Exercise E5.1. The height of the polygon is strictly less than its width.

- E5.2 (**Monotonic evolution of \mathcal{H}_{dc} and \mathcal{H}_{sp}**). Prove the facts relative to statements (ii) and (iii) in Theorem 5.5.

Hint: Make use of the optimality of the Voronoi partition and of center locations stated in Propositions 2.19 and 2.21.

- E5.3 (**Correctness of Lmtd-Vrn-cntrd**). Prove Theorem 5.5(v).

Hint: To establish the monotonic evolution of the multicenter function, make use of the optimality of the Voronoi partition stated in Proposition 2.13 and of the centroid locations stated in Proposition 2.15. To establish the convergence result, make use of the LaSalle Invariance Principle stated in Theorem 1.19.

- E5.4 (**Correctness of Rng-Vrn-cntrd**). Mimic the proof of Theorem 5.5(iv) to show that the evolutions of RNG-VRN-CNTRD monotonically optimize the mixed distortion-area multicenter function

$$\mathcal{H}_{\text{dist-area}, \frac{\pi}{2}, b}, \quad \text{with } b = -\text{diam}(Q)^2,$$

and asymptotically approach its set of critical points.

- E5.5 (**The “n-bugs problem” and cyclic interactions: cont’d**). Consider n robots at counterclockwise-ordered positions $\theta_1, \dots, \theta_n$. First, consider the cyclic balancing system described in Exercise E1.30 with parameter $k = 1/4$, and given by

$$\theta_i(\ell + 1) = \frac{1}{4}\theta_{i+1}(\ell) + \frac{1}{2}\theta_i(\ell) + \frac{1}{4}\theta_{i-1}(\ell), \quad \ell \in \mathbb{Z}_{\geq 0}.$$

Second, consider the Voronoi-centroid law on the circle (with uniform density) in which each robot computes its Voronoi partition of the circle (see Figure 2.5) and then moves to the midpoint of its arc. Show that the two behaviors are identical.

Bibliography

- Agarwal, P. K. and Sharir, M. [1998] *Efficient algorithms for geometric optimization*, ACM Computing Surveys, **30**(4), 412–458.
- Arkin, R. C. [1998] *Behavior-Based Robotics*, MIT Press, ISBN 0262011654.
- Arsie, A., Savla, K., and Frazzoli, E. [2009] *Efficient routing algorithms for multiple vehicles with no explicit communications*, IEEE Transactions on Automatic Control, to appear.
- Astolfi, A. [1999] *Exponential stabilization of a wheeled mobile robot via discontinuous control*, ASME Journal on Dynamic Systems, Measurement, and Control, **121**(1), 121–127.
- Balch, T. and Parker, L. E., (editors) [2002] *Robot Teams: From Diversity to Polymorphism*, A. K. Peters, ISBN 1568811551.
- Batalin, M. A. and Sukhatme, G. S. [2004] *Coverage, exploration and deployment by a mobile robot and communication network*, Telecommunication Systems Journal, **26**(2), 181–196, Special Issue on Wireless Sensor Networks.
- Bertsekas, D. P. and Tsitsiklis, J. N. [1997] *Parallel and Distributed Computation: Numerical Methods*, Athena Scientific, ISBN 1886529019.
- Boltyanski, V., Martini, H., and Soltan, V. [1999] *Geometric methods and optimization problems*, volume 4 of *Combinatorial optimization*, Kluwer Academic Publishers, ISBN 0792354540.
- Bulusu, N., Heidemann, J., and Estrin, D. [2001] *Adaptive beacon placement*, in *International Conference on Distributed Computing Systems*, pages 489–498, Mesa, AZ.
- Burgard, W., Moors, M., Stachniss, C., and Schneider, F. E. [2005] *Coordinated multi-robot exploration*, IEEE Transactions on Robotics, **21**(3), 376–386.
- Caicedo-Nùñez, C. H. and Žefran, M. [2008] *Performing coverage on non-convex domains*, in *IEEE Conf. on Control Applications*, pages 1019–1024, San Antonio, TX.

- Choset, H. [2001] *Coverage for robotics – A survey of recent results*, Annals of Mathematics and Artificial Intelligence, **31**(1-4), 113–126.
- Chvátal, V. [1975] *A combinatorial theorem in plane geometry*, Journal of Combinatorial Theory. Series B, **18**, 39–41.
- Cortés, J. [2008] *Area-constrained coverage optimization by robotic sensor networks*, in *IEEE Conf. on Decision and Control*, pages 1018–1023, Cancún, México.
- Cortés, J. and Bullo, F. [2005] *Coordination and geometric optimization via distributed dynamical systems*, SIAM Journal on Control and Optimization, **44**(5), 1543–1574.
- Cortés, J., Martínez, S., and Bullo, F. [2005] *Spatially-distributed coverage optimization and control with limited-range interactions*, ESAIM: Control, Optimisation & Calculus of Variations, **11**, 691–719.
- Cortés, J., Martínez, S., Karatas, T., and Bullo, F. [2004] *Coverage control for mobile sensing networks*, IEEE Transactions on Robotics and Automation, **20**(2), 243–255.
- de Silva, V. and Ghrist, R. [2007] *Coverage in sensor networks via persistent homology*, Algebraic & Geometric Topology, **7**, 339–358.
- Drezner, Z., (editor) [1995] *Facility Location: A Survey of Applications and Methods*, Series in Operations Research, Springer, ISBN 0-387-94545-8.
- Du, Q., Faber, V., and Gunzburger, M. [1999] *Centroidal Voronoi tessellations: Applications and algorithms*, SIAM Review, **41**(4), 637–676.
- Dynia, M., Kutyłowski, J., Meyer auf der Heide, F., and Schindelhauer, C. [2006] *Smart robot teams exploring sparse trees*, in *International Symposium of Mathematical Foundations of Computer Science*, Stará Lesná, Slovakia.
- Efrat, A. and Har-Peled, S. [2006] *Guarding galleries and terrains*, Information Processing Letters, **100**(6), 238–245.
- Eidenbenz, S., Stamm, C., and Widmayer, P. [2001] *Inapproximability results for guarding polygons and terrains*, Algorithmica, **31**(1), 79–113.
- Fraigniaud, P., Gąsieniec, L., Kowalski, D. R., and Pelc, A. [2004] *Collective tree exploration*, in *LATIN 2004: Theoretical Informatics*, M. Farach-Colton, editor, volume 2976 of *Lecture Notes in Computer Science*, pages 141–151, Springer, ISBN 3540212582.
- Ganguli, A., Cortés, J., and Bullo, F. [2007] *Distributed coverage of nonconvex environments*, in *Networked Sensing Information and Control (Proceedings of the NSF Workshop on Future Directions in Systems Research*

- for *Networked Sensing, May 2006, Boston, MA*), V. Saligrama, editor, pages 289–305, Lecture Notes in Control and Information Sciences, Springer, ISBN 0387688439.
- Gao, C., Cortés, J., and Bullo, F. [2008] *Notes on averaging over acyclic digraphs and discrete coverage control*, Automatica, **44**(8), 2120–2127.
- Ghosh, S. K. [1987] *Approximation algorithms for Art Gallery Problems*, in *Proceedings of the Canadian Information Processing Society*, pages 429–434.
- Graham, R. and Cortés, J. [2009] *Asymptotic optimality of multicenter Voronoi configurations for random field estimation*, IEEE Transactions on Automatic Control, **54**(1), 153–158.
- Gupta, V., Chung, T. H., Hassibi, B., and Murray, R. M. [2006] *On a stochastic sensor selection algorithm with applications in sensor scheduling and sensor coverage*, Automatica, **42**(2), 251–260.
- Hernández-Peñalver, G. [1994] *Controlling guards*, in *Canadian Conference on Computational Geometry*, pages 387–392, Saskatoon, Canada.
- Howard, A., Matarić, M. J., and Sukhatme, G. S. [2002] *Mobile sensor network deployment using potential fields: A distributed scalable solution to the area coverage problem*, in *International Conference on Distributed Autonomous Robotic Systems*, pages 299–308, Fukuoka, Japan.
- Howard, A., Parker, L. E., and Sukhatme, G. S. [2006] *Experiments with a large heterogeneous mobile robot team: Exploration, mapping, deployment, and detection*, International Journal of Robotics Research, **25**(5-6), 431–447.
- Hussein, I. I. and Stipanović, D. M. [2007] *Effective coverage control for mobile sensor networks with guaranteed collision avoidance*, IEEE Transactions on Control Systems Technology, **15**(4), 642–657.
- Kwok, A. and Martínez, S. [2009] *Deployment algorithms for a power-constrained mobile sensor network*, International Journal on Robust and Nonlinear Control, to appear.
- Laventall, K. and Cortés, J. [2009] *Coverage control by robotic networks with limited-range anisotropic sensory*, International Journal of Control, **82**(6), 1113–1121.
- Lee, D. T. and Lin, A. K. [1986] *Computational complexity of art gallery problems*, IEEE Transactions on Information Theory, **32**(2), 276–282.
- Lekien, F. and Leonard, N. E. [2009] *Non-uniform coverage and cartograms*, SIAM Journal on Control and Optimization, **48**(1), 351–372.

- Lloyd, S. P. [1982] *Least squares quantization in PCM*, IEEE Transactions on Information Theory, **28**(2), 129–137, presented as Bell Laboratory Technical Memorandum at a 1957 Institute for Mathematical Statistics meeting.
- Martínez, S. [2009] *Distributed interpolation schemes for field estimation by mobile sensor networks*, IEEE Transactions on Control Systems Technology, to appear.
- Martínez, S., Bullo, F., Cortés, J., and Frazzoli, E. [2007] *On synchronous robotic networks – Part II: Time complexity of rendezvous and deployment algorithms*, IEEE Transactions on Automatic Control, **52**(12), 2214–2226.
- Okabe, A., Boots, B., Sugihara, K., and Chiu, S. N. [2000] *Spatial Tesselations: Concepts and Applications of Voronoi Diagrams*, second edition, Wiley Series in Probability and Statistics, John Wiley, ISBN 0471986356.
- Pavone, M., Frazzoli, E., and Bullo, F. [2008] *Distributed policies for equitable partitioning: Theory and applications*, in *IEEE Conf. on Decision and Control*, pages 4191–4197, Cancún, México.
- Payton, D., Daily, M., Estowski, R., Howard, M., and Lee, C. [2001] *Pheromone robotics*, Autonomous Robots, **11**(3), 319–324.
- Pimenta, L. C. A., Kumar, V., Mesquita, R. C., and Pereira, G. A. S. [2008] *Sensing and coverage for a network of heterogeneous robots*, in *IEEE Conf. on Decision and Control*, pages 3947–3952, Cancún, México.
- Pinciu, V. [2003] *A coloring algorithm for finding connected guards in art galleries*, in *Discrete Mathematical and Theoretical Computer Science*, volume 2731/2003 of *Lecture Notes in Computer Science*, pages 257–264, Springer.
- Poduri, S. and Sukhatme, G. S. [2004] *Constrained coverage for mobile sensor networks*, in *IEEE Int. Conf. on Robotics and Automation*, pages 165–172, New Orleans, LA.
- Rekleitis, I. M., Dudek, G., and Milios, E. [2001] *Multi-robot collaboration for robust exploration*, Annals of Mathematics and Artificial Intelligence, **31**(1-4), 7–40.
- Schultz, A. C. and Parker, L. E., (editors) [2002] *Multi-Robot Systems: From Swarms to Intelligent Automata*, Kluwer Academic Publishers, ISBN 1402006799, Proceedings from the 2002 NRL Workshop on Multi-Robot Systems.
- Schwager, M., Bullo, F., Skelly, D., and Rus, D. [2008] *A ladybug exploration strategy for distributed adaptive coverage control*, in *IEEE Int. Conf. on Robotics and Automation*, pages 2346–2353, Pasadena, CA.

- Schwager, M., Rus, D., and Slotine, J. J. [2009] *Decentralized, adaptive coverage control for networked robots*, International Journal of Robotics Research, **28**(3), 357–375.
- Simmons, R., Apfelbaum, D., Fox, D., Goldman, R., Haigh, K., Musliner, D., Pelican, M., and Thrun, S. [2000] *Coordinated deployment of multiple heterogenous robots*, in *IEEE/RSJ Int. Conf. on Intelligent Robots & Systems*, pages 2254–2260, Takamatsu, Japan.
- Skyum, S. [1991] *A simple algorithm for computing the smallest enclosing circle*, Information Processing Letters, **37**(3), 121–125.
- Susca, S., Martínez, S., and Bullo, F. [2009] *Gradient algorithms for polygonal approximation of convex contours*, Automatica, **45**(2), 510–516.
- Zhong, M. and Cassandras, C. G. [2008] *Distributed coverage control in sensor network environments with polygonal obstacles*, in *IFAC World Congress*, pages 4162–4167, Seoul, Korea.

share May 20, 2009

Algorithm Index

VRN-CNTRD ALGORITHM	10
VRN-CNTRD-DYNMCS ALGORITHM	10
VRN-CRCMCNTR ALGORITHM	12
VRN-NCNTR ALGORITHM	13
LMTD-VRN-NRML ALGORITHM	14
LMTD-VRN-CNTRD ALGORITHM	15
RELATIVE-SENSING LMTD-VRN-CNTRD ALGORITHM	16
RNG-VRN-CNTRD ALGORITHM	16

share May 20, 2009

Subject Index

- control and
 - communication law [12](#)
 - “away-from-closest-neighbor”, [13](#)
 - “move-toward-furthest-vertex”, [13](#)
- limited-Voronoi-centroid, [15](#)
- Limited-Voronoi-normal, [14](#)
- Voronoi-centroid, [10](#)
 - on planar vehicles, [10](#)
 - range-limited version of, [16](#)
- Voronoi-circumcenter, [8](#)
- Voronoi-incenter, [13](#)
- coordination task deployment
 - ε - r -area, [7](#)
 - ε - r -distortion-area, [7](#)
 - ε -disk-covering, [8](#)
 - ε -distortion, [7](#)
 - ε -sphere-packing, [8](#)
- density, [6](#)
- function
 - area, [7](#)
 - disk-covering, [8](#)
 - distortion, [7](#)
 - mixed distortion-area, [8](#)
 - sphere-packing, [8](#)
- matrix
 - tridiagonal augmented, [29](#)
- performance, [7](#)
- problem
 - n -bugs, [32](#)
 - Art Gallery, [24](#)
- unicycle, [10](#)
- vensor, [26](#)
- Voronoi configuration
 - r -limited centroidal, [7](#)
 - centroidal, [7](#)
 - circumcenter, [8](#)
 - incenter, [8](#)

share May 20, 2009

Symbol Index

- $\mathcal{CC}_{\text{VRN-CNTRD}}$: Voronoi-centroid control and communication law, 10
 $\mathcal{CC}_{\text{VRN-CNTRD-DYNMCS}}$: Voronoi-centroid control and communication law on planar vehicles, 10
 $\mathcal{CC}_{\text{VRN-CRCMCNTR}}$: Voronoi-circumcenter control and communication law, 12
 $\mathcal{CC}_{\text{VRN-NCNTR}}$: Voronoi-incenter control and communication law, 13
 $\mathcal{CC}_{\text{LMTD-VRN-NRML}}$: limited-Voronoi-normal control and communication law, 14
 $\mathcal{CC}_{\text{LMTD-VRN-CNTRD}}$: limited-Voronoi-centroid control and communication law, 15
 $\mathcal{CC}_{\text{RNG-VRN-CNTRD}}$: range-limited version of Voronoi-centroid control and communication law, 16
 $\mathcal{T}_{\varepsilon\text{-sp-dply}}$: ε -sphere-packing deployment task, 8
 $\mathcal{T}_{\varepsilon\text{-distor-dply}}$: ε -distortion deployment task, 7
 $\mathcal{T}_{\varepsilon\text{-r-area-dply}}$: $\varepsilon\text{-r-area}$ deployment task, 7
 $\mathcal{T}_{\varepsilon\text{-r-distor-area-dply}}$: $\varepsilon\text{-r-distor-area}$ deployment task, 7
 $\mathcal{T}_{\varepsilon\text{-dc-dply}}$: ε -disk-covering deployment task, 8
 $\text{vers} : \mathbb{R}^d \rightarrow \mathbb{R}^d$: versor operator, 26